Journal of Orthopaedic Translation 35 (2022) 62–71

Contents lists available at ScienceDirect

Journal of Orthopaedic Translation

journal homepage: www.journals.elsevier.com/journal-of-orthopaedic-translation

Rotator cuff repair with biodegradable high-purity magnesium suture anchor in sheep model

Yudie Chen [a,1], Yu Sun [b,1], Xinhui Wu [a], Jie Lou [b], Xiaonong Zhang [b,c,**], Zhaoxiang Peng [a,*]

[a] The Affiliated Lihuili Hospital, Ningbo University, Ningbo, 315100, China
[b] State Key Laboratory of Metal Matrix Composites, School of Materials Science and Engineering, Shanghai Jiao Tong University, Shanghai, 200240, China
[c] Suzhou Origin Medical Technology Co. Ltd., Jiangsu, 215513, China

ARTICLE INFO

Keywords:
High-purity magnesium
Suture anchor
Rotator cuff repair
Sheep model

ABSTRACT

Background: Rotator cuff tear has become one of the diseases affecting people's living quality. Conventional anchor materials such as titanium alloy and poly-lactic acid can lead to postoperative complications like bone defects and aseptic inflammation. Magnesium (Mg)-based implants are biodegradable and biocompatible, with strong potential to be applied in orthopaedics.

Methods: In this study, we developed a high-purity (HP) Mg suture anchor and studied its mechanical properties and degradation behavior in vitro. Furthermore, we described the use of high-purity Mg to prepare suture anchor for the rotator cuff repair in sheep.

Results: The in vitro tests showed that HP Mg suture anchor possess proper degradation behavior and appropriate mechanical property. Animal experiment indicated that HP Mg suture anchor provided reliable anchoring function in 12 weeks and showed no toxic effect on animal organs.

Conclusion: In summary, the HP Mg anchor presented in this study had favorable mechanical property and biosecurity.

The translational potential of this article: The translational potential of this article is to use high-purity Mg to develop a degradable suture anchor and verify the feasibility of the application in animal model. This study provides a basis for further research on the clinical application of biodegradable high-purity Mg suture anchor.

1. Introduction

Rotator cuff tear is the most common disease that causes shoulder pain and limitation of activity [1–3]. With the development of population aging, rotator cuff tear has gradually become a social health problem that cannot be ignored [4]. Without surgical intervention, tendon-bone structure cannot regenerate once it is injured. Surgery acquires more significant improvement in pain and function compared to non-surgical treatment for full-thickness rotator cuff tear. Thus, rotator cuff repair with suture anchor is widely used in clinical practice.

Suture anchor made of titanium and its alloys has remarkable mechanical properties. However, titanium is an inert metal that cannot be degraded leading to the need for a second surgery to remove the implant when there are complications [5,6]. Besides, prolonged implantation may release a variety of harmful ions, leading to the risk of inflammation and allergies. Third, the stress shielding effects caused by the high Young's modulus may cause bone loss. PEEK is a highly popular suture anchor used by many clinicians due to its radiolucency, mechanical properties and chemical resistance, but its biological inertness limits osseointegration [7]. Biodegradable materials such as poly-lactic acid have become popular choice with the development of material sciences. But a large number of acidic molecules or oligomers will be produced in the process of degradation [8], which will stimulate the surrounding tissues and lead to more serious inflammatory reaction, even effusion, cysts, etc. [9,10]. Therefore, new materials own effectiveness and biosafety are needed in the clinical practice of rotator cuff repair.

* Corresponding author.
** Corresponding author. State Key Laboratory of Metal Matrix Composites, School of Materials Science and Engineering, Shanghai Jiao Tong University, Shanghai, 200240, China.
E-mail addresses: nbchyd@163.com (Y. Chen), sandynote@sjtu.edu.cn (Y. Sun), 815380964@qq.com (X. Wu), jokerlxy@sjtu.edu.cn (J. Lou), xnzhang@sjtu.edu.cn (X. Zhang), pzxao@hotmail.com (Z. Peng).
[1] Co-first authors: These authors contributed equally to this work.

https://doi.org/10.1016/j.jot.2022.07.008
Received 31 March 2022; Received in revised form 1 July 2022; Accepted 21 July 2022

Magnesium is one of the most representative biodegradable metals, having excellent biodegradability, mechanical properties and biocompatibility [11–14]. It has a lower standard electrode potential than hydrogen and can be degraded into harmless products including Mg ions and hydrogen gas in an aqueous solution under standard conditions. It has a higher mechanical strength compared to the natural bone and a similar Young's modulus relative to cortical bone [15,16]. These unique properties make Mg reduce stress shielding during application besides provide strong fixation. Besides, Mg can promote bone formation by stimulating osteoblasts and endothelial cells [17,18]. Mg is one of the essential elements of the human body and involved in more than 300 enzyme reactions in bone and plays an important role in formation and regeneration of bone. In addition, Mg generates fewer artifacts in CT compared to titanium [19,20], which is beneficial to postoperative follow-up. In addition, Zhang et al. [21] revealed a previously undefined role of magnesium in promoting CGRP-mediated osteogenic differentiation and Zheng et al. [22] found fibrosis could be targeted by augmenting CGRP expression to accelerate fracture healing.

Huang et al. [23] fixed femoral neck fracture with weight-bearing screws prepared with high-purity(HP) Mg in goats. The long-term follow-up observation shows the screws degraded by approximately 10% at 4 weeks and 38.8% at 12 weeks. Guo et al. [24] found the degradation rate of HP magnesium interbody cage was rapid within the first 3 weeks after implantation surgery at goat cervical spine. In view of the characteristic of tendon-bone healing, the initial four weeks is pivotal.

Therefore, in this study, we applied 99.98% HP magnesium (HP Mg) suture anchor to the sheep model of rotator cuff repair with biocomposite suture anchor as the control to verify the effectiveness and safety of HP Mg as a suture anchor material and provide a basis for further research on HP Mg suture anchor.

2. Materials and methods

2.1. Materials preparation

Samples of suture-anchor made of high purity magnesium (99.98 wt.%) were supplied by Suzhou Origin Medical Technology Co. Ltd., China. The anchors were designed according to the drawing in Fig. 1, where they have a total length of 14.5 mm, shaft outer diameter of 4.4 mm, shaft inner diameter of 3.0 mm, and pitch of 1.90 mm. Samples of biocomposite suture-anchor (BioComposite Corkscrew FT) purchased from Arthrex, USA, were used as control. All samples were rinsed in acetone and ethanol successively, washed in distilled water, and then sterilized with 29 kGy of 60Co radiation.

2.2. In vitro experiments

2.2.1. Immersion tests

HP Mg suture anchors were immersed in PBS solution (Sinopharm Chemical ReagentCo., Ltd, China) pH = 7.4 for 14 days at 37 °C. The degradation performance of the suture anchors was presented by the amount of hydrogen released during degradation and the weight loss. In brief, collected the hydrogen generated during the degradation progress through an inverted burette. And the time point of hydrogen evolution during the immersion experiment was set for statistics. The mass of the anchors before and after immersion was measured by the analytical balance (METLER TOLEDO, Zurich).

2.2.2. Surface morphology analysis

The surface morphology of HP Mg suture anchors was observed by a scanning electron microscope (SEM, Nova nanosem 230, USA). After suture anchors were degraded in PBS, the samples were coated with gold to observe the corrosion products layer. Then the corroded suture anchors were ultrasonically cleaned in a solution containing 200 g/l CrO3 and 10 g/l AgNO3, and absolute ethanol for 5 min to remove corrosion products on the surface of the suture anchors. Finally, observe the surface morphology of degraded HP Mg suture anchor.

2.2.3. Pullout force and torsion tests of HP Mg suture anchor

The pullout force test setup is shown in Fig. 2. The suture line used in test was #2 FiberWire. A synthetic bone of solid (supplied by Suzhou Origin Medical Technology Co. Ltd., China) was fixed on a sample stage. A hole with a 4.4 mm diameter was drilled in the synthetic bone, and then screwed the HP Mg suture anchor. A material testing machine (Zwick, Germany) was used for the mechanical evaluation of the constructions. The torsion test was carried out on an HP Mg suture anchor with an axial preloading load of 2.00 N at a constant rate of 3.00 rpm in a torsion test machine (Paratronix, China). HP Mg suture anchors before and after being immersed in PBS for 14 days were both measured. Three samples were used for each test.

2.3. Animal study

2.3.1. Sheep model of rotator cuff repair

Six skeletally mature, male sheep were used as the rotator cuff repair model. The study protocol was approved by the Ethics Committee for Animal Research of Hangzhou caiyang Animal Husbandry Co., LTD (reference number 202004101021). Sheep were randomly divided into the HP Mg group and the Biocomposite group. No.1 to No.3 were in HP Mg group and No.4 to No.6 were in biocomposite group.

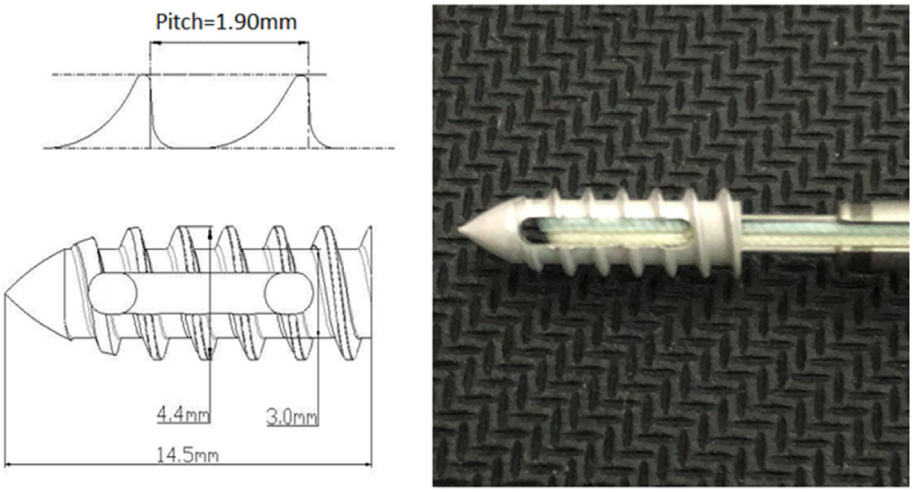

Fig. 1. The processing drawing and picture of HP Mg suture anchor.

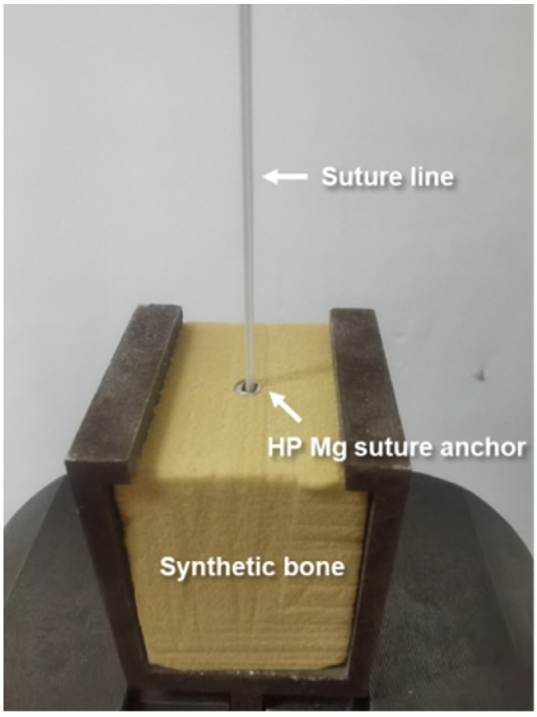

Fig. 2. Schematic of pullout force test setup.

Sheep were fasted for 24 h before surgery and then placed in the left position and under anesthesia with Lu-mian-ning (2 mg/kg). The right shoulder was shaved and disinfected routinely and then covered with disposable surgery sheet. An arc-shaped incision was made at the shoulder joint through the skin and subcutaneous fascia. The anterior margin of the deltoid was separated by blunt dissection and pulled to the rear to expose the tendon of the infraspinatus. The distal of the tendon of the infraspinatus was cut by scalpel and the footprint was exposed. A screw tap was used to drill bone tunnel and a HP Mg suture anchor or a biocomposite suture anchor was twisted into the bone tunnel. Then, the tendon of the infraspinatus was seamed with Mason–Allen stitch technique. Finally, the incision was closed in layers. Lu-xing-ning (2 mg/kg) was used to awaken the sheep, and prophylactic antibiotics were administered for 3 days (see Fig. 3).

2.3.2. Serological study

Serum Mg ion, liver function and kidney function tests were performed on each sheep at 1 day, 3 days, 7 days, 14 days and 28 days after surgery. Blood samples were collected from the jugular vein of each sheep. Serum Mg ion, liver function and kidney function were tested by an automatic biochemical-immune analyzer (Beckman Coulter AU5800, USA). Liver function was evaluated by ALT (glutamic pyruvic transaminase) and serum albumin levels, while kidney function was evaluated by serum creatinine level.

2.3.3. Imaging evaluation

The sheep were anesthetized to obtain CT images at 4w, 8w and 12w postoperative and MR images at 1day pre-operation and 1day 4w, 8w and 12w postoperative. CT scans were performed with a CT scanner (Brilliance 16, Philips, NED).

MRI scans were performed with a 3.0 T MR scanner (Discovery MR750, GE Medical Systems, USA). According to Sugaya et al. [25], postoperative cuff integrity was classified into 5 categories using different views of T2-weighted images. Type I, cuff has sufficient thickness with uniform low intensity; Type II, sufficient thickness with partial high intensity; Type III, insufficient thickness without discontinuity; Type IV, presence of minor discontinuity; and Type V, presence of a major discontinuity on each image.

2.3.4. Histology study

One sheep from each group was euthanized by injecting an overdose of anaesthetic at 4w, 8w and 12w after surgery. Tendon-bone tissue, heart, liver and kidney specimens were harvested and then fixed in 10% buffered formalin for 24 h. Tendon-bone tissue was cut into 5 mm

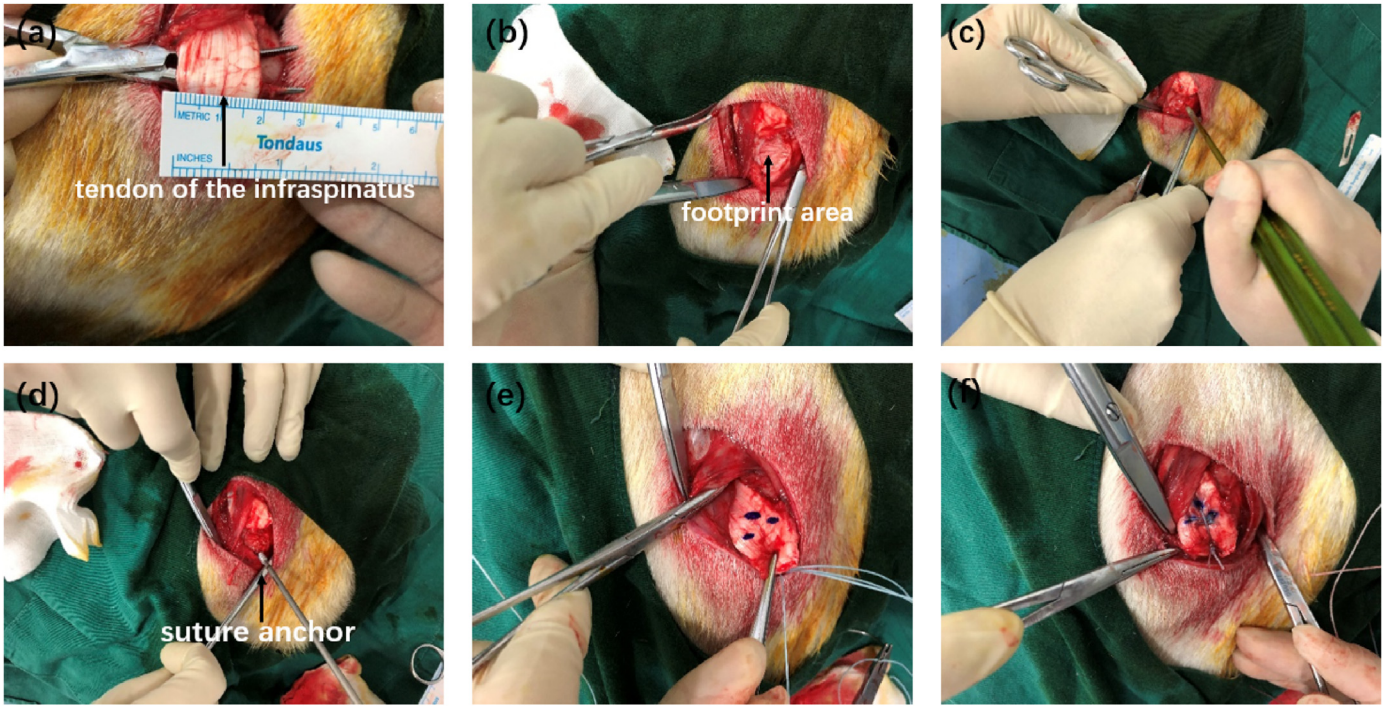

Fig. 3. The surgical process of rotator cuff repair. (**a**): Exposed the tendon of the infraspinatus; (**b**): Cut the distal of the tendon and exposed footprint; (**c**): Drilled bone tunnel with screw tap; (**d**)–(**f**): Seamed the tendon with Mason–Allen stitch technique.

thickness slices, decalcified in EDTA (pH 7.2) for 4 weeks after fixed, dehydrated and embedded routinely. It must be pointed out that the implant was removed before decalcification to avoid effects of degradation products of implants. At last, samples were cut with thickness of 4 μm and stained with hematoxylin and eosin (HE) and hematoxylin phosphotungstate (PATH).

2.4. Statistical analysis

In this paper, the statistical analysis was performed with SPSS software (v 22; IBM). The repeated ANOVA was used for comparison of serum Mg, liver and kidney function between HP Mg and biocomposite group. The graphs were created with GraphPad Prism (v 8.0.2; GraphPad Software Inc).

3. Results

3.1. Immersion experiments

To further evaluate the degradation behavior of the HP Mg suture anchor, samples were immersed in PBS solution for 14 days. The amount of hydrogen evolution, weight loss of the suture anchors was measured. As shown in Fig. 4(a), the rate of hydrogen release in the first 12 h is much faster than later. Fig. 4(b) shows that the hydrogen release in the first 12 h accounts for 2/5 of the total hydrogen release in the 14 days. It illustrates that when a layer of corrosion products is formed on the surface of the magnesium implant, the corrosion rate will be significantly reduced.

In the weight loss test, the weight of HP Mg suture anchors was 124.633 ± 0.643 mg. After being immersed in PBS for 14 days, the weight of suture anchors reduced to 113.567 ± 1.955 mg. In addition, the weight loss rate was 8.879 ± 1.124%. It is easy to find that the standard deviation of the suture anchors increased after immersion compares to before immersion. From this side, it reveals that the degradation of suture anchors has certain individual differences (see Fig. 5).

3.2. Surface morphology

Fig. 6 shows the same partial photograph, located inside of the HP Mg suture anchor where the rate of corrosion here is relative fast due to crevice corrosion [26,27], before and after being immersed in PBS for 14 days. The image on the right is a partial enlargement of the image on the left. Fig. 6(a-d) shows the surface morphology of the sample is smooth before degradation. While acicular degradation products were generated on the surface after the sample was degraded. Washed these products away, fluvial corrosion marks were observed on the surface of the sample. Pits appeared where corrosion is more severe. In brief, the surface morphology of the samples changed greatly before and after degradation.

3.3. Mechanical properties

The pullout force of HP Mg suture anchor measured by setup shown in Fig. 7 revealed that when the pullout force reached 297.67 ± 24.00 N, the anchors were not pulled out of the synthetic bone while the suture broke. There is no significant between samplers before or after being immersed in PBS for 14 days. That means that degraded for 14 days HP Mg suture anchor still can withstand enough tension to meet the requirements of fixation in vivo. As shown in Fig. 7 (b), the maximum torque of HP Mg suture is 0.25 ± 0.01 Nm, while it decreased to 0.13 ± 0.01 Nm after degradation ($p < 0.01$). Nevertheless, anchors do not require high torque, demonstrating a better material candidate for HP Mg as potential biodegradable fixators in the field of joint repair.

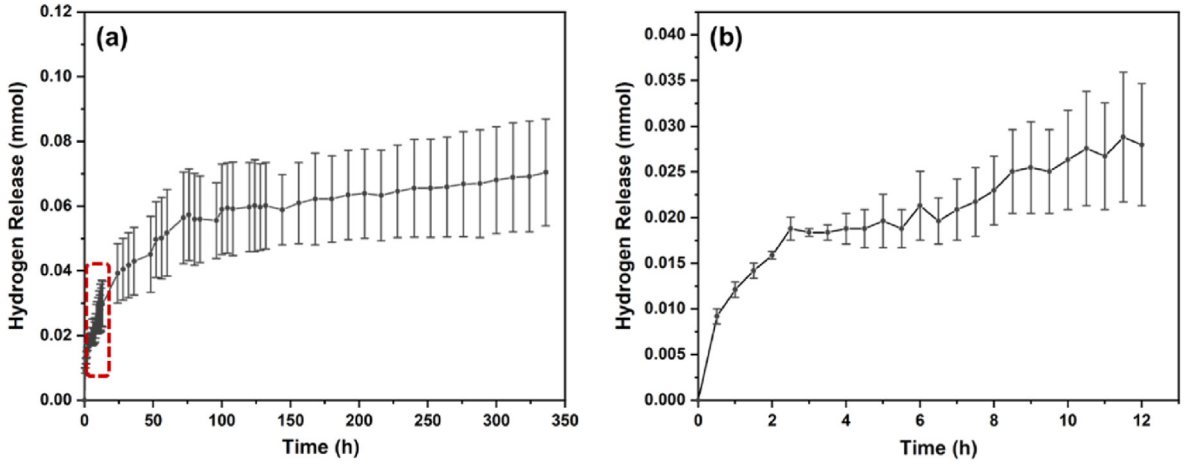

Fig. 4. The hydrogen evolution volume of HP Mg suture anchor immersed in PBS solution for 14 days. (**b**) Is the part magnification of (**a**).

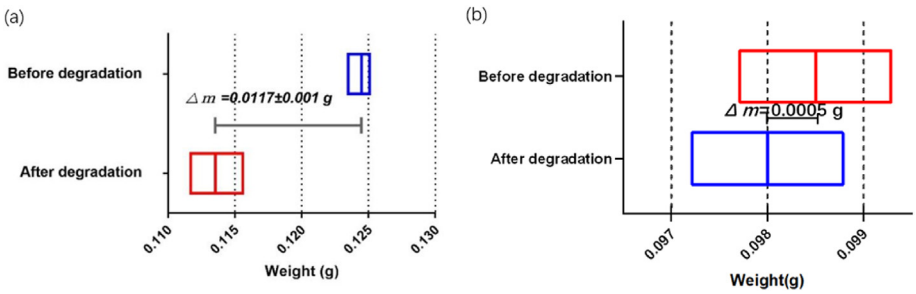

Fig. 5. The weight loss of HP Mg suture anchor ((a)) and biocomposite suture anchor ((b)) immersed in PBS solution for 14 days.

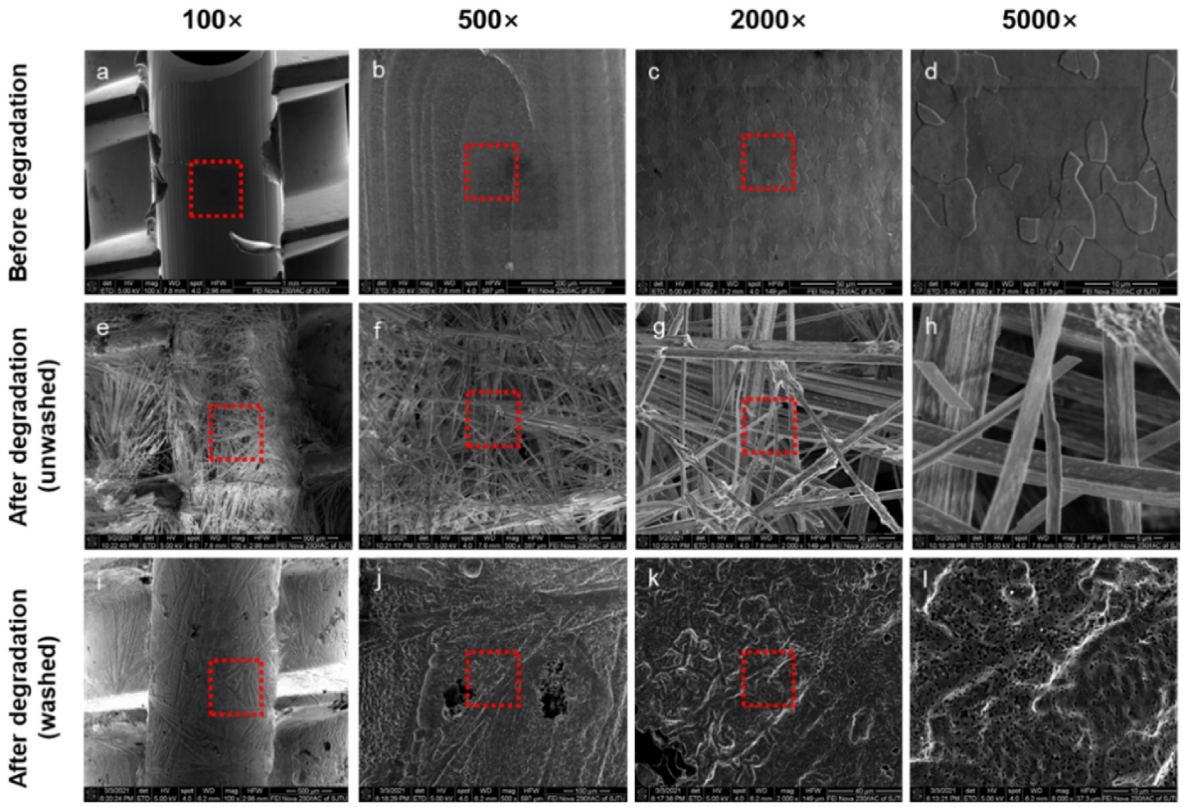

Fig. 6. The surface morphology of HP Mg suture anchor before(**a**)-(**d**) and after(**e**)-(**l**) degradation in PBS solution for 14 days.

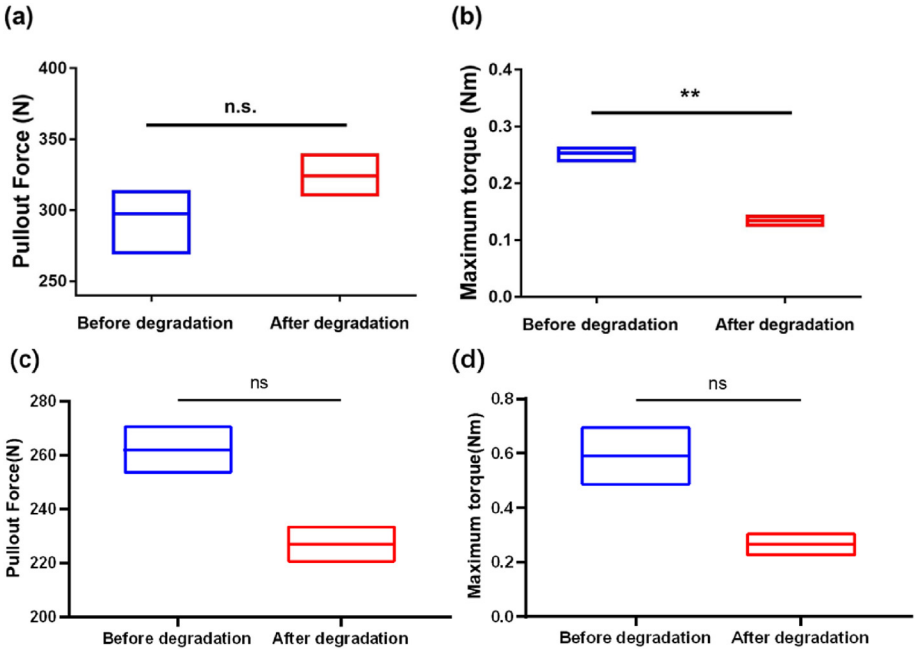

Fig. 7. The pullout force and maximum torque of HP Mg suture anchor ((a)and (b)) and biocomposite suture anchor ((c)and (d)) before and after degradation in PBS solution for 14 days.

3.4. Serology study

Serum Mg + concentration of samples collected at 1, 3, 7, 14 and 28 days after surgery showed no significant difference between HP Mg group and biocomposite group. There was also no significant difference in liver and kidney functions between two groups. Though observe fluctuation can be observed, all samples showed similar trends (see Fig. 8). These results suggested the implantation of HP Mg suture anchor did not cause Mg metabolism disorder and disorder of liver and kidney function.

3.5. Imaging evaluation

The CT images showed obvious low-density cavity around suture

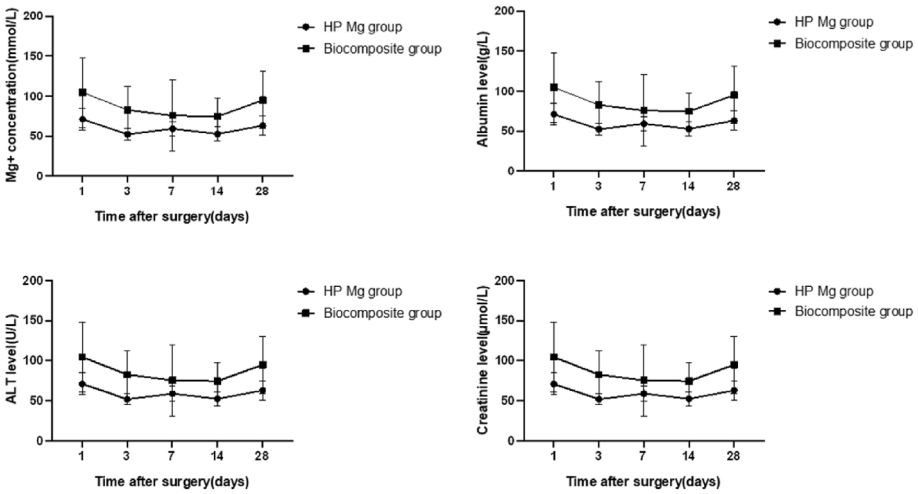

Fig. 8. The serological indicators of samples obtained at 1, 3, 7, 14 and 28 days after surgery. All samples showed similar trends while there was obvious fluctuation.

anchor in HP Mg group at 4 weeks after surgery. Meanwhile, in biocomposite group, there was no cavity around suture anchor. By preliminary measurement of volume of suture anchor and cavity, it is observed that both HP Mg and biocomposite suture anchor degraded after surgery and cavity around HP Mg suture anchor showed no obvious change in following 8 weeks. Furthermore, all suture anchor maintained basic structure after 12 weeks (see Fig. 9).

According to Sugaya et al. [25], MRI showed all shoulders with type I integrity at 1 days, 4 weeks, 8 weeks and 12 weeks after surgery. It suggests both HP Mg suture anchor and biocomposite suture anchor provide reliable anchoring action during 12 weeks after surgery (see Fig. 10).

3.6. Histology study

Fig. 11(a) shows the heart, liver and kidney specimens harvested at 12 weeks after surgery. In general view, organs from two groups show normal organizational structure. Comparing to biocomposite group, histological structure of organs from HP Mg group shows no obvious change. Besides, the inflammatory cell infiltration and accumulation of hazardous substances was not observed. In brief, the implantation of HP Mg suture anchor showed no toxic effect on animal organs.

Fig. 11(b) shows the tendon-bone tissue harvested at 4w, 8w and 12w after surgery. At 4weeks after surgery, tendon was tightly bound to bone in two groups and the inflammatory cell infiltration was not observed. Histological sections at 4 weeks and 8 weeks also showed good bond of bone and tendon and no local inflammatory response. It suggested HP Mg suture anchor had no negative effect to the physiological repair process of tendon-bone tissue.

4. Discussion

Recently, researchers have conducted extensive studies on the development of magnesium-based orthopedic implants [28–32]. Mg is a biodegradable metal with good biocompatibility and young's modulus close to natural cortical bone, so it is widely regarded as an ideal

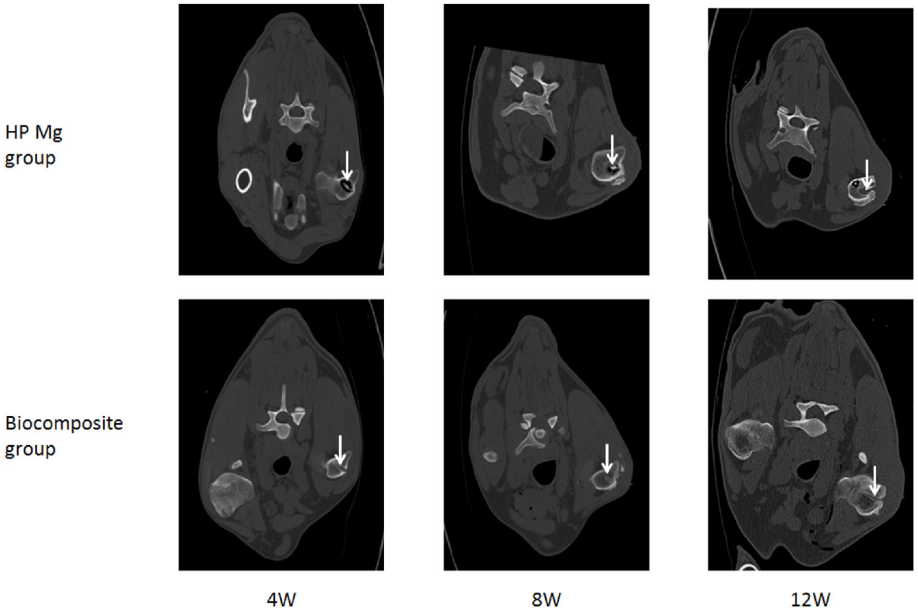

Fig. 9. The CT images of the humerus and suture anchor. In HP Mg group (**a**, **b** and **c**), obvious low-density cavity around suture anchor observed at 4 weeks after surgery and showed no distinct change in following 8 weeks. Meanwhile, there was no cavity in biocomposite group (**d**, **e** and **f**). The anchor is located where the arrow indicates.

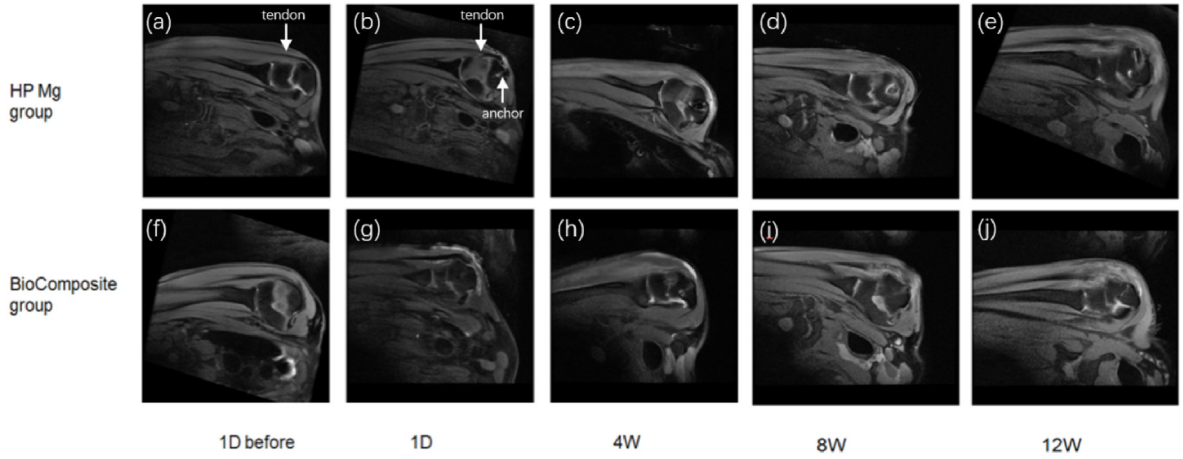

Fig. 10. The MRI show shoulders with type I integrity during 12 weeks after surgery According to Sugaya et al. [25].

orthopedic implant material. However, rapid degradation is a major limitation of its clinical application. In general, high purity magnesium degrades more slowly than magnesium alloy and it has better biosafety with no alloying elements [33,34]. So, in this study, we used high purity magnesium to prepare the anchor.

In vitro tests, we found that the hydrogen release was rapidly during the first 12 h and it accounted for about 2/5 of the total. In the initial stage, HP Mg suture anchor was completely exposed to the solution and rapid degradation was inhibited with the formation of degradation products. Acicular degradation products can be observed on the surface after the sample was degraded. Washed these products away, uniform corrosion marks appeared and anchor maintained the integrity of the overall structure after immersed in PBS solution for 14 days, the weight loss rate of HP Mg suture anchor was 8.879 ± 1.124%. In the existing in vitro studies of pure magnesium, weight loss rates after immersed for 14days ranged from 2% to 8% in different buffers [35]. The weight loss rate of HP suture anchor was relatively high due to its large surface area. The amount of hydrogen released showed that degradation mainly occurred in the first 12 h. In addition, there was no loss of structural integrity. In summary, HP Mg suture anchor had a uniform degradation behavior and a slow degradation rate in vitro during 2 weeks.

The pullout force test showed that when the force reached 297.67 ± 24.00 N, the suture broke while the anchors were not pulled out of the synthetic bone. It suggested HP Mg suture anchor had sufficient mechanical strength and was bound tightly to the synthetic bone. According to Qi et al. [36], the failure load of titanium screw anchor was 328.45 ± 89.58 N. There is no definite conclusion on the minimum load required after rotator cuff repair, Mazzocca et al. [37] determined that its minimum failure load was 250 N. Besides, there is no literature report on the torque test of suture anchor. Besides, there was no damage during screwing, indicating that the HP Mg suture anchor had ideal torque. Therefore, considering the mechanical properties, HP Mg suture anchor is a suitable choice for repairing rotator cuff.

In this study, a biodegradable HP Mg suture anchor was applied to rotator cuff repair in a large animal for the first time. We chose sheep as research object because of the similar size, bone structure and remodeling of the infraspinatus tendon to the human supraspinatus tendon [38,39]. Survival times was set at 12 weeks to verify the efficacy and biosafety of HP Mg suture anchor.

After surgery, all the sheep were ambulatory with no local infections or movement limitations. MRI scans were performed at 1day preoperation and 1day, 4w, 8w and 12w postoperative. Images showed shoulders with type I integrity during 12 weeks. Besides, tendon-bone tissue specimens were harvested at 4w, 8w and 12w after surgery and histological sections showed good bond of bone and tendon and no local inflammatory response. It indicated that, in contrast to biocomposite suture anchor, HP Mg suture anchor also could provide reliable anchoring function and did not cause local inflammation in 12 weeks.

The biosafety of long-term implantation is also an important factor for clinical use. The serum Mg + concentration, liver and kidney functions were detected at 1 day, 3 days, 7 days, 14 days and 28 days after surgery. Though fluctuation could be observed, indexes were within normal range and there was no significant difference between the two groups. Moreover, histological sections of heart, liver and kidney specimens harvested at 4 weeks, 8 weeks and 12 weeks showed normal physiological structure and no inflammatory cell infiltration and accumulation of hazardous substances was not observed. The results manifested that the implantation of HP Mg suture anchor was safe in 12 weeks, which is consistent with the results of several magnesium-based metal related in vivo experiments [40–42].

As reported in several studies [43–45], gas cavities could be observed around HP Mg suture anchor as early as 4 weeks after surgery. Rapid and excessive gas production can lead to implant failure and raise the risk of gas embolism. However, it has not been found in relevant studies that this phenomenon affects local osteogenesis or overall function, and the cavity gradually shrinks as the bone grows into the cavity. Wang et al. [46] reported gas produced by Mg–Zn–Zr alloy can cause cavitation within cancellous bone at 2 weeks after implantation and confirmed the gas cavities did not affect osteogenesis of Mg alloy by Micro-CT and histological examination. The cause of cavity formation has not been determined. It is believed that the gas appears within the cavities is continuously exchanged with dissolved gases surrounding tissues and blood. Therefore, controlling the degradation rate of implants is an effective way to prevent the formation of gas cavities. There have been numerous surface treatment methods studied to control the degradation behavior [47–50], but effective methods still need to be further studied before clinical application.

Besides, as a biodegradable material, bone ingrowth should be considered in the degradation process. The bone conductivity of the material is closely related to this, which is one of the main reasons for the development of biocomposite suture anchors by incorporating calcium phosphates. Factors affecting bone conduction contain material stiffness, wettability, surface biochemical structure, structural agent, and surface morphology. Therefore, these factors should be considered in the design.

Due to this study was a preliminary study on the application of magnesium suture anchor in vivo, there were some limitations. First of all, the sample size of animals is small. Secondly, we set 12 weeks as the timepoint, which is usually more suitable for small to medium sized animal models. In the future, a larger sample size and longer experimental period are necessary. Besides, we will consider do in-depth research and discussion the mechanism of gas cavities formation.

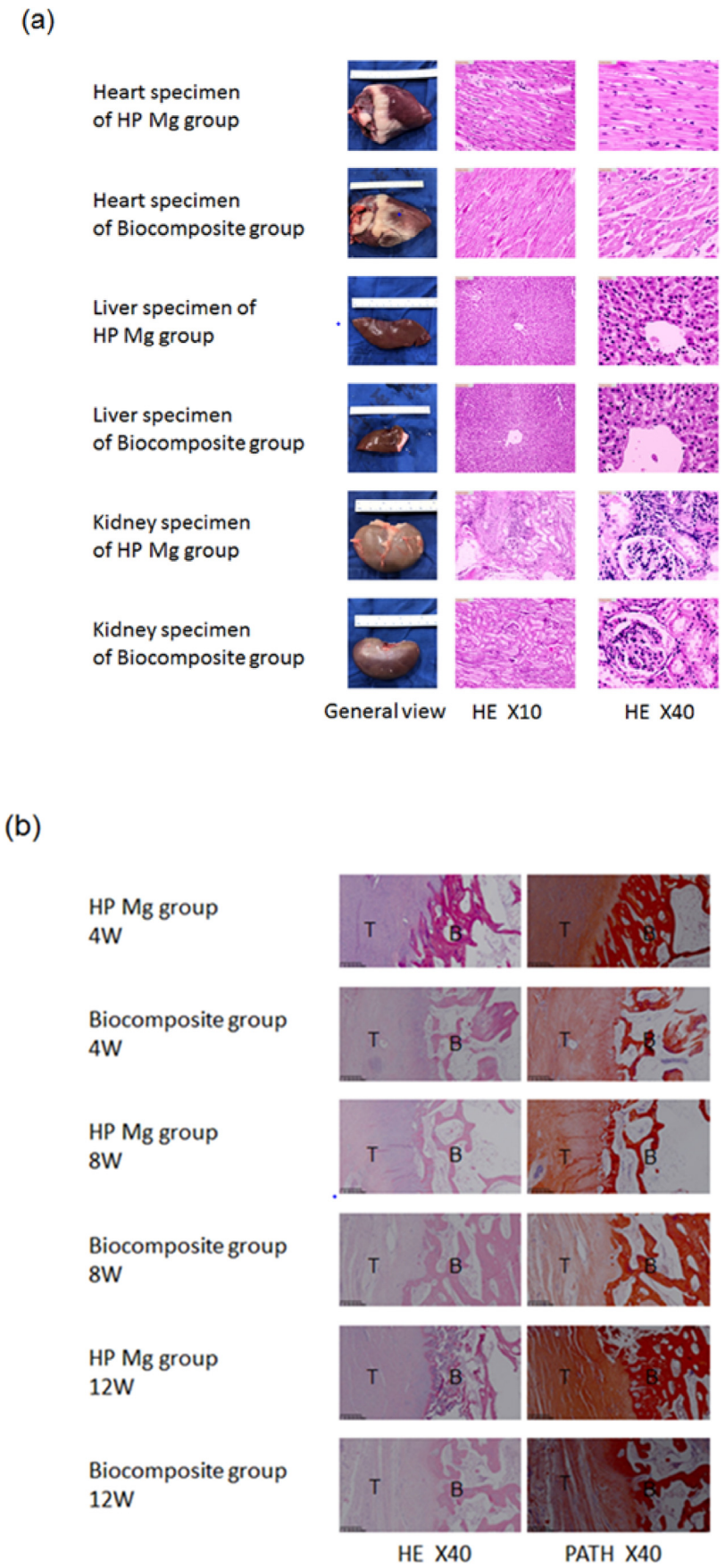

Fig. 11. Histological analysis of the organs and tendon-bone tissue. (**a**) General view and representative HE stained sections of heart, liver and kidney at 12 weeks after surgery. (**b**) Representative HE and PATH-stained sections of tendon-bone tissue (T represents tendon repaired, B represents bone).

5. Conclusions

In this paper, we prepared suture anchor with HP Mg (99.98 wt.%). In vitro, degradation behavior and mechanical property were tested. We also applied HP Mg suture anchor to the sheep model of rotator cuff repair with biocomposite suture anchor as the control to study efficacy and biosafety. The following conclusions can be drawn.

HP Mg suture anchor showed proper degradation behavior in vitro tests. HP Mg suture anchor showed rapid degradation at an early stage, especially in the first 12 h, then performed uniform and slow degradation in the following time. Acicular degradation products were observed after the sample was degraded and the surface of the sample showed uniform fluvial corrosion marks after they were washed away.

HP Mg suture anchor showed appropriate mechanical property before and after degradation. Sample possessed enough bonding strength with the synthetic bone and maintained strength after degradation for 14 days. In addition, sample showed proper torque.

In the sheep model of rotator cuff repair, HP Mg suture anchor provided reliable anchoring function in 12 weeks and showed no toxic effect on animal organs. HP Mg suture anchor produced gas cavities around the anchor during degradation, but no negative effects on implant fixation and tendon-bone healing were observed in 12 weeks.

HP Mg suture anchor has the potential to be developed as a novel internal device for rotator cuff repair. Future research should focus on the mechanism of gas cavities formation and methods to reduce and avoid it.

Author contributions

Designing the experiments, Y.C. and Y.S.; performing the experiments, Y.C., Y.S., X.W.and J.L.; contributing the reagents, materials and analysis tools, X.Z. and Z.P.; analyzing the data, Y.C. and Y.S.; writing—original draft preparation, Y.C. and Y.S.; writing—review and editing, X.Z. and Z.P.; project administration, X.Z. and Z.P.; funding acquisition, Z.P. All authors have read and agreed to the published version of the manuscript.

Funding

sThis work was supported by the “Science and Technology Innovation 2025” Major Special Project of Ningbo (No. 2019B10064), Zhejiang Provincial Natural Science Foundation of China under Grant (No. LGF21H060003), Programs Supported by the Ningbo Natural Science Foundation (2018A610203, 202002N3195, a grant from the National Natural Science Foundation of China (81,401,819) and the foundation project for medical science and technology of Zhejiang Province (2022KY1083).

Declaration of competing interest

We declare that we have no financial and personal relationships with other people or organizations that can inappropriately influence our work, there is no professional or other personal interest of any nature or kind in any product, service and/or company that could be construed as influencing the position presented in, or the review of, the manuscript entitled.

References

[1] Snedeker JG, Foolen J. Tendon injury and repair - a perspective on the basic mechanisms of tendon disease and future clinical therapy. Acta Biomater 2017;63:18–36.
[2] Keener JD, Patterson BM, Orvets N, Chamberlain AM. Degenerative rotator cuff tears: refining surgical indications based on natural history data. J Am Acad Orthop Surg 2019;27(5):156–65.
[3] Cederqvist S, Flinkkila T, Sormaala M, Ylinen J, Kautiainen H, Irmola T, et al. Non-surgical and surgical treatments for rotator cuff disease: a pragmatic randomised clinical trial with 2-year follow-up after initial rehabilitation. Ann Rheum Dis 2021;80(6):796–802.
[4] Tashjian RZ. Epidemiology, natural history, and indications for treatment of rotator cuff tears. Clin Sports Med 2012;31(4):589–604.
[5] Jacobs JJ, Hallab NJ, Skipor AK, Urban RM. Metal degradation products: a cause for concern in metal-metal bearings? Clin Orthop Relat Res 2003;417:139–47.
[6] Wang JL, Xu JK, Hopkins C, Chow DH, Qin L. Biodegradable magnesium-based implants in orthopedics-A general review and perspectives. Adv Sci 2020;7(8):1902443.
[7] Lee JW, Han HS, Han KJ, Park J, Jeon H, Ok MR, et al. Long-term clinical study and multiscale analysis of in vivo biodegradation mechanism of Mg alloy. Proc Natl Acad Sci U S A 2016;113(3):716–21.
[8] Grun NG, Holweg PL, Donohue N, Klestil T, Weinberg AM. Resorbable implants in pediatric fracture treatment. Innov. Surg. Sci. 2018;3(2):119–25.
[9] Douglas Matijakovich, Solomon David, Benitez Carlos L, Huang Hsin-Hui, Poeran Jashvant, Berger Natalie, et al. Long-term follow-up of perianchor cyst formation after rotator cuff repair. JSES Int. 2021;5:863–8.
[10] Sgroi M, Friesz T, Schocke M, Reichel H, Kappe T. Biocomposite suture anchors remain visible two years after rotator cuff repair. Clin Orthop Relat Res 2019;477(6):1469–78.
[11] Zhao D, Witte F, Lu F, Wang J, Li J, Qin L. Current status on clinical applications of magnesium-based orthopaedic implants: a review from clinical translational perspective. Biomaterials 2017;112:287–302.
[12] Noviana D, Paramitha D, Ulum MF, Hermawan H. The effect of hydrogen gas evolution of magnesium implant on the postimplantation mortality of rats. J. Orthop. Translat. 2016;5:9–15.
[13] Song B, Li W, Chen Z, Fu G, Li C, Liu W, et al. Biomechanical comparison of pure magnesium interference screw and polylactic acid polymer interference screw in anterior cruciate ligament reconstruction-A cadaveric experimental study. J. Orthop. Translat. 2017;8:32–9.
[14] Mau JR, Hawkins KM, Woo SL, Kim KE, McCullough MBA. Design of a new magnesium-based anterior cruciate ligament interference screw using finite element analysis. J. Orthop. Translat. 2020;20:25–30.
[15] Rendenbach C, Fischer H, Kopp A, Schmidt-Bleek K, Kreiker H, Stumpp S, et al. Improved in vivo osseointegration and degradation behavior of PEO surface-modified WE43 magnesium plates and screws after 6 and 12 months. Mater. Sci. Eng. C Mater. Biol. Appl. 2021;129:112380.
[16] Julmi S, Kruger AK, Waselau AC, Meyer-Lindenberg A, Wriggers P, Klose C, et al. Processing and coating of open-pored absorbable magnesium-based bone implants. Mater. Sci. Eng. C Mater. Biol. Appl. 2019;98:1073–86.
[17] Zhao Z, Li G, Ruan H, Chen K, Cai Z, Lu G, et al. Capturing magnesium ions via microfluidic hydrogel microspheres for promoting cancellous bone regeneration. ACS Nano 2021;15(8):13041–54.
[18] Ye L, Xu J, Mi J, He X, Pan Q, Zheng L, et al. Biodegradable magnesium combined with distraction osteogenesis synergistically stimulates bone tissue regeneration via CGRP-FAK-VEGF signaling axis. Biomaterials 2021;275:120984.
[19] Filli L, Luechinger R, Frauenfelder T, Beck S, Guggenberger R, Farshad-Amacker N, et al. Metal-induced artifacts in computed tomography and magnetic resonance imaging: comparison of a biodegradable magnesium alloy versus titanium and stainless steel controls. Skeletal Radiol 2015;44(6):849–56.
[20] Sonnow L, Konneker S, Vogt PM, Wacker F, von Falck C. Biodegradable magnesium Herbert screw - image quality and artifacts with radiography, CT and MRI. BMC Med Imag 2017;17(1):16.
[21] Zhang Y, Xu J, Ruan YC, Yu MK, O'Laughlin M, Wise H, et al. Implant-derived magnesium induces local neuronal production of CGRP to improve bone-fracture healing in rats. Nat Med 2016;22(10):1160–9.
[22] N. Zheng, J. Xu, Y.C. Ruan, L. Chang, X. Wang, H. Yao, et al, Magnesium facilitates the healing of atypical femoral fractures: a single-cell transcriptomic study, Mater Today 52 (2022) 43-62.
[23] Huang S, Wang B, Zhang X, Lu F, Wang Z, Tian S, et al. High-purity weight-bearing magnesium screw: translational application in the healing of femoral neck fracture. Biomaterials 2020;238:119829.
[24] Guo X, Xu H, Zhang F, Lu F. Bioabsorbable high-purity magnesium interbody cage: degradation, interbody fusion, and biocompatibility from a goat cervical spine model. Ann Transl Med 2020;8(17):1054.
[25] Sugaya H, Maeda K, Matsuki K, Moriishi J. Functional and structural outcome after arthroscopic full-thickness rotator cuff repair: single-row versus dual-row fixation. Arthroscopy 2005;21(11):1307–16.
[26] Chen B, Wu H, Yi R, Wang W, Xu H, Zhang S, et al. In vitro crevice corrosion of biodegradable magnesium in different solutions. J Mater Sci Technol 2020;52:83–8.
[27] Wu H, Zhang C, Lou T, Chen B, Yi R, Wang W, et al. Crevice corrosion - a newly observed mechanism of degradation in biomedical magnesium. Acta Biomater 2019;98:152–9.
[28] Kozakiewicz M. Are magnesium screws proper for mandibular condyle head osteosynthesis? Materials 2020;13(11).
[29] Kawamura N, Nakao Y, Ishikawa R, Tsuchida D, Iijima M. Degradation and biocompatibility of AZ31 magnesium alloy implants in vitro and in vivo: a micro-computed tomography study in rats. Materials 2020;13(2).
[30] Sheikh Z, Najeeb S, Khurshid Z, Verma V, Rashid H, Glogauer M. Biodegradable materials for bone repair and tissue engineering applications. Materials 2015;8(9):5744–94.
[31] Gigante A, Setaro N, Rotini M, Finzi SS, Marinelli M. Intercondylar eminence fracture treated by resorbable magnesium screws osteosynthesis: a case series. Injury 2018;49(Suppl 3):S48–53.
[32] Plaass C, von Falck C, Ettinger S, Sonnow L, Calderone F, Weizbauer A, et al. Bioabsorbable magnesium versus standard titanium compression screws for fixation of distal metatarsal osteotomies - 3 year results of a randomized clinical trial. J Orthop Sci 2018;23(2):321–7.

[33] Zhao D, Huang S, Lu F, Wang B, Yang L, Qin L, et al. Vascularized bone grafting fixed by biodegradable magnesium screw for treating osteonecrosis of the femoral head. Biomaterials 2016;81:84–92.
[34] Cheng P, Han P, Zhao C, Zhang S, Wu H, Ni J, et al. High-purity magnesium interference screws promote fibrocartilaginous entheses regeneration in the anterior cruciate ligament reconstruction rabbit model via accumulation of BMP-2 and VEGF. Biomaterials 2016;81:14–26.
[35] Walker J, Shadanbaz S, Kirkland NT, Stace E, Woodfield T, Staiger MP, et al. Magnesium alloys: predicting in vivo corrosion with in vitro immersion testing. J Biomed Mater Res B Appl Biomater 2012;100(4):1134–41.
[36] Guo Q, Li C, Qi W, Li H, Lu X, Shen X, et al. A novel suture anchor constructed of cortical bone for rotator cuff repair: a biomechanical study on sheep humerus specimens. Int Orthop 2016;40(9):1913–8.
[37] Mazzocca AD, Millett PJ, Guanche CA, Santangelo SA, Arciero RA. Arthroscopic single-row versus double-row suture anchor rotator cuff repair. Am J Sports Med 2005;33(12):1861–8.
[38] Ahmad Z, Al-Wattar Z, Rushton N. Tissue engineering for the ovine rotator cuff: surgical anatomy, approach, implantation and histology technique, along with review of literature. J Invest Surg 2020;33(2):147–58.
[39] Turner AS. Experiences with sheep as an animal model for shoulder surgery: strengths and shortcomings. J Shoulder Elbow Surg 2007;16(5 Suppl):S158–63.
[40] Klima K, Ulmann D, Bartos M, Spanko M, Duskova J, Vrbova R, et al. A complex evaluation of the in-vivo biocompatibility and degradation of an extruded ZnMgSr absorbable alloy implanted into rabbit bones for 360 days. Int J Mol Sci 2021; 22(24).
[41] Thormann U, Alt V, Heimann L, Gasquere C, Heiss C, Szalay G, et al. The biocompatibility of degradable magnesium interference screws: an experimental study with sheep. BioMed Res Int 2015;2015:943603.
[42] Yu W, Zhao H, Ding Z, Zhang Z, Sun B, Shen J, et al. In vitro and in vivo evaluation of MgF2 coated AZ31 magnesium alloy porous scaffolds for bone regeneration. Colloids Surf B Biointerfaces 2017;149:330–40.
[43] Razavi M, Fathi M, Savabi O, Tayebi L, Vashaee D. Biodegradable magnesium bone implants coated with a novel bioceramic nanocomposite. Materials 2020;13(6).
[44] Antoniac I, Adam R, Bita A, Miculescu M, Trante O, Petrescu IM, et al. Comparative assessment of in vitro and in vivo biodegradation of Mg-1Ca magnesium alloys for orthopedic applications. Materials 2020;14(1).
[45] Holweg P, Berger L, Cihova M, Donohue N, Clement B, Schwarze U, et al. A lean magnesium-zinc-calcium alloy ZX00 used for bone fracture stabilization in a large growing-animal model. Acta Biomater 2020;113:646–59.
[46] Wang J, Jiang H, Bi Y, Sun J, Chen M, Liu D. Effects of gas produced by degradation of Mg-Zn-Zr Alloy on cancellous bone tissue. Mater. Sci. Eng. C Mater. Biol. Appl. 2015;55:556–61.
[47] Gao F, Hu Y, Gong Z, Liu T, Gong T, Liu S, et al. Fabrication of chitosan/heparinized graphene oxide multilayer coating to improve corrosion resistance and biocompatibility of magnesium alloys. Mater. Sci. Eng. C Mater. Biol. Appl. 2019; 104:109947.
[48] Mehrjou B, Dehghan-Baniani D, Shi M, Shanaghi A, Wang G, Liu L, et al. Nanopatterned silk-coated AZ31 magnesium alloy with enhanced antibacterial and corrosion properties. Mater. Sci. Eng. C Mater. Biol. Appl. 2020;116:111173.
[49] Rahman M, Dutta NK, Choudhury NR. Microroughness induced biomimetic coating for biodegradation control of magnesium. Mater. Sci. Eng. C Mater. Biol. Appl. 2021;121:111811.
[50] Zhang Y, Lin T, Meng H, Wang X, Peng H, Liu G, et al. 3D gel-printed porous magnesium scaffold coated with dibasic calcium phosphate dihydrate for bone repair in vivo. J. Orthop. Translat. 2022;33:13–23.